Adv. J. Sci. Eng.

Advanced Journal of Science and Engineering

https://adv-j-sci-eng.com
eISSN: 2717-0705

Original Research

Mechanical and Thermal Properties of Extruded Thermoplastic Polyester Elastomer/TiO₂ Nano-Composites: Effect of Surface Modification

Haydar U. Zaman[1,✉], **Ruhul A. Khan**[1]

[1]*Institute of Radiation and Polymer Technology, Bangladesh Atomic Energy Commission, Savar, Dhaka, Bangladesh*

✉*Corresponding Author*: K. Silas; *Email*: haydarzaman07@gmail.com; *ORCID*: 0000-0002-1673-6915

Advanced Journal of Science and Engineering. 2022;3(2):136-145. https://doi.org/10.22034/advjse22032136

Received: 24 April 2022 / ***Revised***: 09 May 2022 / ***Accepted***: 14 May 2022 / ***Published***: 15 May 2022

Abstract: Nano-titanium dioxide (titania, $nTiO_2$) reinforced polymer composites develop new ways of engineering that exhibit better mechanical and chemical properties. This work investigates the effects of nanoparticles and compatibilizer (maleated styrene ethylene butylene styrene, SEBSMA) on the features of poly(butylene terephthalate)-block-tetramethylene ether glycol terephthalate (PBT-TEGT)-based thermoplastic polyester elastomer (TPE). The $nTiO_2$ particle content in the TPE was varied from 3 to 7 wt%. $nTiO_2$ particles were coated with SEBSMA before melt blending for better surface adhesion and fine dispersion. The influences of uncoated and coated $nTiO_2$ particles with varying concentrations on the mechanical and thermal features of binary TPE/$nTiO_2$ nanocomposites were manufactured by the melt compounding process tracked by hot press mold. Due to the rigid structure of $nTiO_2$ particles, all tensile features (yield strength, tensile strength, and tensile modulus) increased while elongation at break reduced. It probably requires better compatibility of $nTiO_2$ with SEBSMA and in this case, due to the formation of $nTiO_2$ finer with TPE, has been persuasive to ensure lower elongation results. DSC measurements showed that the inclusion of coated $nTiO_2$ resulted in higher crystallization temperature and melting temperature than virgin TPE. Furthermore, the addition of coated $nTiO_2$ particles enhances the overall mechanical features and thermal behaviors such as the thermal stability of the material.

Keywords: Thermoplastic polyester elastomer; Nano-TiO_2; Nanocomposites; Mechanical properties; Thermal properties.

Introduction

Thermoplastic elastomers (TEs) are inventive ingredients, which increase the importance of a boundary cover between rubber ingredients and plastics. To date, various TEs based on styrene, urethane, amide, olefin, and ester have been commercialized, with automotive parts and household appliances having their uses [1-4]. With TEs, a thermoplastic polyester elastomer (TPE), which consists of poly(butylene terephthalate) (PBT) as the hard part and tetramethylene ether glycol terephthalate (TEGT) as the soft part, has superior mechanical, thermal properties, and elasticity

[5]. TPEs in TEs have very good low-temperature flexibility and high performance for mechanical properties at temperatures up to 130 °C [6]. It has excellent oil resistance, impact, creep, and abrasion and is also used for automotive parts such as gears and sprockets, tubing, electronics, electronic parts, and even increasingly substitute the cross-linked rubbers [7]. It has attracted interest because of its low specific gravity and excellent reprocessing, which has been considered an environmentally friendly material that replaces vulcanized rubber and PVC. Consequently, both academically and commercially, many studies related to the modification of TPE have progressed to achieve its more suitable features for various applications such as electronic devices, clothing, and outdoor devices, etc. The chemical structure and hydrogen bonding of the PBT-PEGT based TPE is revealed in Scheme 1.

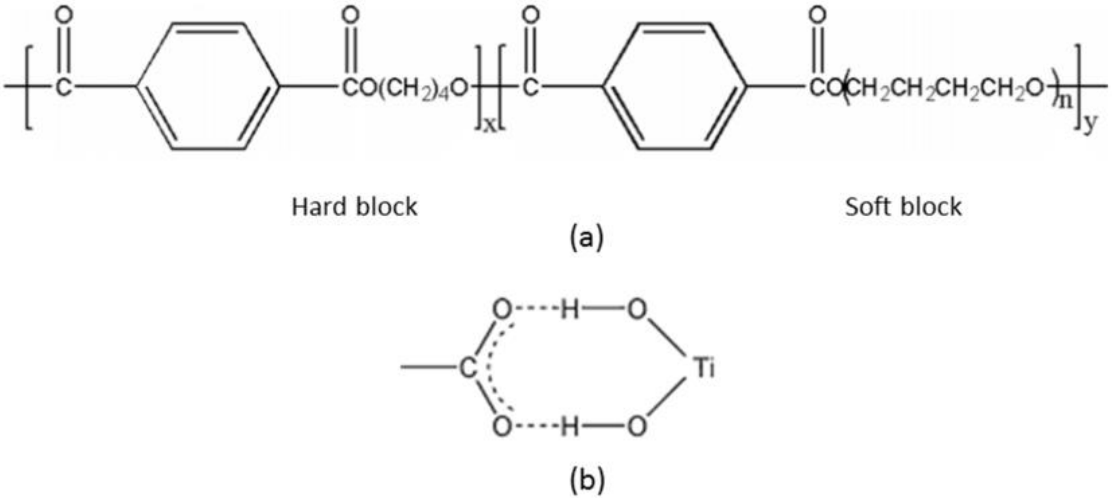

Scheme 1: (a) Chemical structure of thermoplastic polyester elastomer (TPE); (b) binding mode of carboxylate with titania surface: hydrogen bonding.

TE has an elastomeric performance at room temperature, which can be molded at high temperatures identical to common thermoplastic. These ingredients must have great biochemical resistance, stiffness, and color durability to be applied efficiently in practical applications. By carefully mixing thermoplastics with nanoparticles, it is potential to create an operative TPIE component that adapts these appropriate criteria. TPE/nanoparticles nanocomposites continue to arouse great interest in scientists due to their flexibility in design in addition to advanced mechanical features [8]. Inorganic nano-metal oxide (nTiO_2) is one of them because, among all other semiconductor metal oxides families, nTiO_2 is inexpensive, electronic and optical stable, nontoxicity, and corrosion-resistant. The role of nTiO_2 in the matrix can develop the mechanical and thermal features of the matrix due to the small size and large specific areas of the nanoparticles and a potential interfacial bonding between the matrix and the nTiO_2 particles, respectively. The amalgamation of TiO_2 particles into a poly(methyl methacrylate) matrix can substantially affect the features of the matrix [9]. The achieved composites might display enriched mechanical, thermal, or electrical features. Despite a substantial increase in mechanical features, nanoparticles may increase, and nanoparticles may exhibit a decrease in toughness due to their stiffness. To overcome this problem, it is necessary to use dispersants and additive agents [10, 11]. Maleated styrene-ethylene-butylene-styrene (SEBSMA) or maleated polypropylene (PPMA) have been usually used in hybrid composites. Compatibilizers normally reduce the interfacial tensile, increase the interface adhesion, and prevent the coalescence of a component in a blend. Therefore, we can contribute to provide immiscible polymer blends with compatibility and stabilize the morphology of a blend. Tjong et al. [12] used SEBS-g-MA in HDPE/montmorillonite composites. Where SEBS enhanced the toughness of the composite, MA acted as a compatibilizer between montmorillonite particle and HDPE.

In this work, we have prepared TPE/$nTiO_2$ composites by the melt mixing process. In this study, TPE, which is a class of engineering thermoplastic elastomers with a wide range of domestic and industrial applications, is reinforced with SEBAMA coated nanoparticles. The mechanical, morphological, and thermal features of the nanocomposites were investigated according to the $nTiO_2$ particle content and the surface modifier.

Materials and Methods

Materials and Sample Preparation

The polymer matrix TPE granules were kindheartedly delivered by M/S Rupal Plastics Ltd, Mumbai, India with a grade was Hytrel 6356. Nanomaterial such as $nTiO_2$ was supplied by China's Nabond Company. SEBSMA (Kraton, France) was used for modifying particles. Before modification, nano-TiO_2 particles were dried under a vacuum oven. The SEBSMA was dissolved in toluene for two days at 50 °C and then the nanoparticles were slowly incorporated into the solution and mixed with a mechanical mixer (IKA RW 20 digital). The mixer was then crushed after drying for 6 h at a temperature of 50 °C. The quantity of the SEBSMA was 5 wt% of the nanoparticles. The nanocomposite samples were prepared with varying amounts of nanoparticles (3, 5, and 7 wt%), with a fixed amount of 5 wt% of the nanoparticles with compatibilizer (SEBSMA) with a predetermined amount of TPE. The coding of uncoated and coated nanocomposites was as follows: For uncoated, TPE/3 wt% $nTiO_2$ (marked as TPE/3U$nTiO_2$), TPE/5U$nTiO_2$, TPE/7U$nTiO_2$ and for coated, TPE/SEBSMA coated 3 wt% nZnO (designated as TPE/3C$nTiO_2$), TPE/5C$nTiO_2$, TPE/7CTiO_2. The nanoparticles and the TPE were loaded into a Berstorff twin-screw extruder (ZE-25A UTX, KraussMaffei Berstorff GmbH, Germany) with an L/D ratio of 44. The operation temperature was ranged from 180 °C to 220 °C and the speed of the screw was 100 rpm. The extruded strands were ground into small pellets and the achieved pellets were used to make thin plates using a hot press machine.

Characterizations

The tensile test was measured using Shimadzu Universal Testing Machine (model AG-1, Japan). Samples were ~ 10 mm wide, 2 mm thick, with a gauge length of 50 mm. A crosshead speed of 10 mm/min was used to measure the yield strength, tensile strength, tensile modulus, and elongation at break. All experiments were conducted under ASTM-D 638-03, standard [13], and five repeat tests were performed to obtain an average value for each sample. SEM was used to analyze fracture surfaces and the dispersion of nanoparticles. SEM, JSM-6360LV from JEOL, Tokyo, Japan was used to analyze the fracture surfaces of nanocomposites. The samples were gold-coated before imaging. The crystallization and melting behaviors of nanocomposites were investigated by differential scanning calorimetry (DSC, Perkin Elmer DSC-7) in the N_2 atmosphere. Each sample (5-8 mg) was heated from 30 to 240 °C at a heating rate of 10 °C/min and then held at 240 °C to confirm a duplicate thermal history. The sample was cooled down to 30 °C at a cooling rate of 10 °C/min. The thermal stability of the nanocomposites was determined using a thermogravimetric analyzer (TGA, TA Instruments Q500) with a heating rate of 20 °C/min in an N_2 atmosphere. The results were shown to be discussed by the following text.

Results and Discussion

Mechanical Properties of the Nanocomposites

Metal oxide nanoparticles progress the mechanical features of the polymer matrix [14]. Figure 1 illustrates the variation of yield strength and tensile strength of TPE, TPE/UnTiO$_2$ nanocomposites with nTiO$_2$ contents varying from 0 to 7 wt% and TPE/CnTiO$_2$ nanocomposites with the same contents against nTiO$_2$. It can be observed that increasing the nTiO$_2$ content up to 5 wt% increased the yield strength and tensile strength (yield strength increased by 12% and tensile strength increased by 13% for TPE/UnTiO$_2$ nanocomposites and yield strength increased by 23% and tensile strength increased by 24% for TPE/CnTiO$_2$ nanocomposites compared to TPE, respectively) and then decreased by 7 wt%. Increased yield and tensile strength are recognized by mixing the nanofiller spread with the increased properties. The inclusion of nTiO$_2$ particles to the TPE improves the yield and tensile strength of the matrix at 5 wt% nTiO$_2$ due to strong stress transfer from TPE to nTiO$_2$. At 7 wt% of nTiO$_2$ particles, an improvement in yield and tensile strength was reduced due to the relative low-stress transfer effect of nTiO$_2$ particles. In this case, the agglomerated nanoparticles are easily debonded from the TPE and no fraction of the external load is ultimately allowed to reduce the yield and tensile strength. These outcomes were supported by Zaman et al. [15]. To advance the interfacial bonding between nTiO$_2$ particles and TPE, SEBSMA led to the modification of TPE/nTiO$_2$ nanocomposites. The inclusion of SEBSMA in TPE/nTiO$_2$ blends has created significantly noticeable interfacial bonding between filler and matrix than those of TPE/nTiO$_2$ nanocomposites. The maximum yield and tensile strength of the TPE/CnTiO$_2$ nanocomposite were 21.2 MPa and 23.6 MPa at 5 wt% of nTiO$_2$ content, respectively, and about 23% and 24% higher than that the TPE matrix. The increase in the strength of the compatibilized system is expressed by the better distribution produced by the compatibilizer and an enhanced solid-state adherence, which can transfer more stress from the matrix to the dispersion phase. MA functional groups have been grafted into the ethylene butylene mid-block of SEBS. Then, it converts to TPE from SEBSMA molecular chains and bonds with metal oxides. Consequently, homogenous, fine dispersed structures can be achieved.

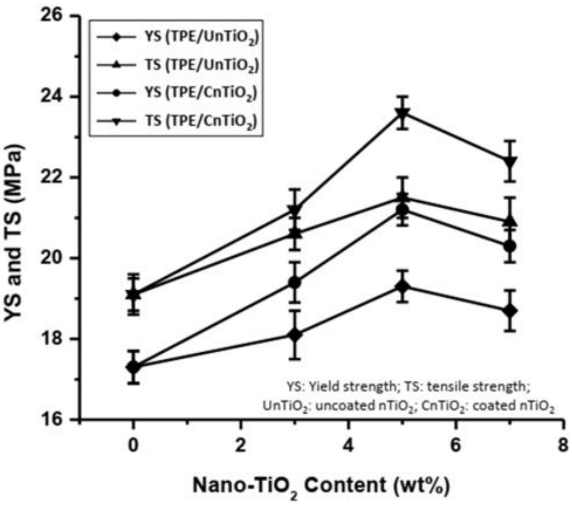

Figure 1: Yield strength and tensile strength of TPE/nTiO$_2$ nanocomposite.

Figure 2 shows the variation of tensile modulus and elongation of TPE/nTiO$_2$ nanocomposites against nTiO$_2$ content. With the inclusion of nTiO$_2$, tensile modulus steadily increased while elongation at break steadily reduced. Modulus growth offers an effective stress transfer from the TPE to nTiO$_2$ particles. On the other hand, the elongation reduced with the inclusion of nTiO$_2$ indicated interference or deformability of TPE by nTiO$_2$. This interference was created by the presence of physical interaction and mechanical restraint of the TPE. Maximum TM (303.8 MPa) of TPE/UnTiO$_2$ nanocomposite was obtained at 7 wt% of nTiO$_2$ content. At this stage, the TM value of the nanocomposite was about 42% higher than that of the TPE matrix. According to the trend of the modulus variant, the TPE/CnTiO$_2$ nanocomposite increased more evidently than TPE/UnTiO$_2$ nanocomposite. Consequently, the elongation at break was reduced with nTiO$_2$ content indicating intervention by nTiO$_2$ in the mobility or deformability of the TPE. This intervention was created by the physical interaction of TPE and the presence of mechanical restraint. As the concentration of the nTiO$_2$ increases, the elongation at break decreased. However, SEBSMA coated nTiO$_2$ nanocomposites showed higher elongation at break than uncoated nTiO$_2$ nanocomposite. The reason for the higher elongation at break is the presence of a soft TPE phase.

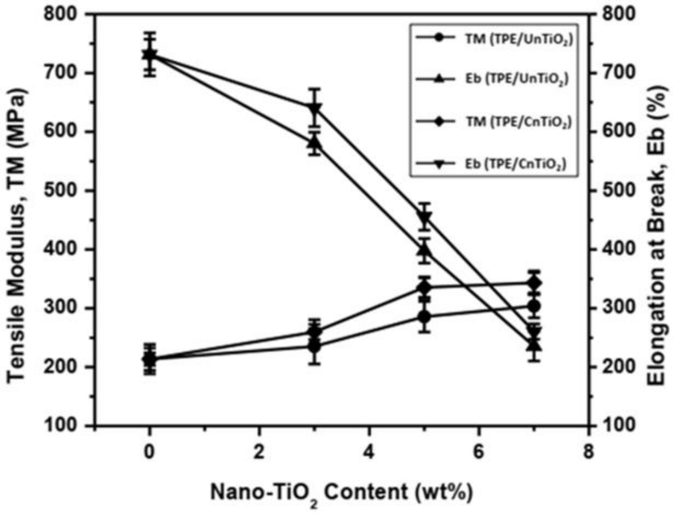

Figure 2: Tensile modulus and elongation at break (%) of TPE/nTiO$_2$ nanocomposites.

Surface Morphology and Particle Dispersion

Mechanical properties are related to the uniformity of multiple morphologies, domain sizes, and shapes to determine the degree of dispersion of interactions between the two stages, and it is considered to be one of the most important elements [16]. Figure 3(a-d) demonstrates the morphological evidence of fractured surfaces of TPE/5UnTiO$_2$, TPE/3CnTiO$_2$, TPE/5CnTiO$_2$ and TPE/7CnTiO$_2$ nanocomposite samples. Figure 3(a) displays that the nTiO$_2$ particles dispersed randomly in TPE/5UnTiO$_2$ and that several large agglomerates with particle size greater than 1 μm were present on the fracture surface, which indicates poor compatibility between TPE and nTiO$_2$. nTIO$_2$ particles were dispersed unevenly in the TPE and lots of particles were agglomerated and conducted into larger cavities around the agglomerates. It makes sense that hydrophilic TiO$_2$ nanoparticles are agglomerated into TPE and the agglomeration increase with the concentration of nTiO$_2$. A specific quantity of hydroxyl groups can form hydrogen bonds between nanoparticles and, as a result, higher agglomeration occurs. Larger nanoparticles are dispersed in TPE/nTiO2 nanocomposite so that there are no functional polymers and thus the interfaces are individually wetted and/or the bonding of the components appears to be somewhat weak. This approves the low tensile properties of the previously discussed nanocomposites. Figure 1(b-d) displays SEM images of TPE/3CnTiO$_2$, TPE/5CnTiO$_2$ and TPE/7CnTiO$_2$ nanocomposites, respectively. The presence of TPE/CnTiO2 changes the morphology. The fractured surface morphology of the TPE/5CnTiO$_2$ nanocomposite was more uniform and finer than that of TPE/3CnTiO$_2$ or TPE/7CnTiO$_2$ nanocomposite, and the mean particle size was smaller than that of TPE/3CnTiO$_2$ or TPE/7CnTiO$_2$ nanocomposite. When the nTiO$_2$ surface was coated with SEBSMA, it dispersed randomly in TPE, avoiding agglomerations and filling cavities, and the interfacial bond between TPE and $nTiO_2$ was improved by the influence of SEBSMA. SEBSMA has covered $nTiO_2$ and improved compatibility between the TPE matrix and $nTiO_2$. These satisfactory nanoparticles and holes can persuade large-scale plastic distortion of the TPE, which increases the strength of the fracture.

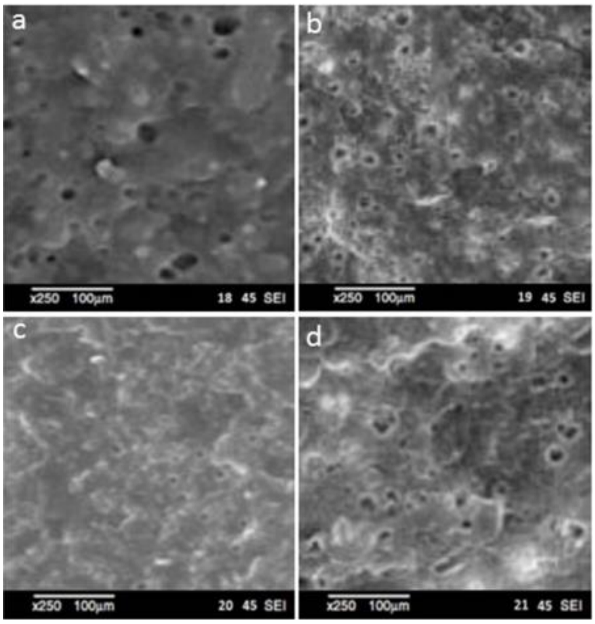

Figure 3: SEM images of TPE/$nTiO_2$ nanocomposites (w/w%) (a) TPE/$5UnTiO_2$, (b) TPE/$3CnTiO_2$, (c) TPE/$5nTiO_2$, and (d) TPE/$7CnTiO_2$.

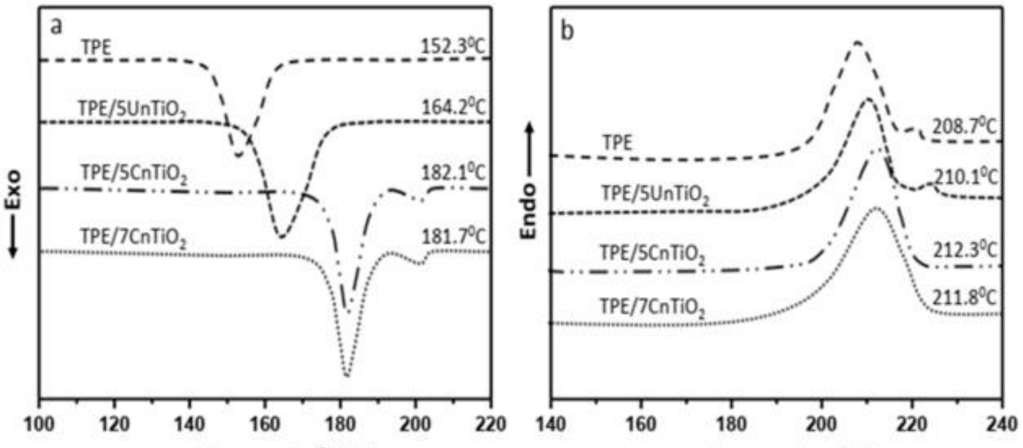

Figure 4: DSC curves of (a) nonisothermal crystallization at a cooling rate of 10 °C/min and (b) second melting process at a heating rate of 10 °C/min for TPE and its nanocomposites.

Thermal Properties of the Nanocomposites

Figure 4 exhibits the DSC thermogram of virgin TPE and its nanocomposites. TPE consists of two partially miscible parts, which are a crystalline hard segment of PBT and the amorphous soft segment of TEGT. From Figure 4(a), the crystallization temperature (T_c) was increased from 152.3 °C of TPE to 164.2 °C of TPE/$5UnTiO_2$ nanocomposite due to heterogeneous nucleation of $nTiO_2$. Significantly, the T_c of TPE/$5CnTiO_2$ increased to 182.1 °C much higher than that of TPE, and even higher TPE/$5UnTiO_2$ gave a special advantage to crystallization and better dispersion of nanoparticles due to the presence of SEBSMA. The interfacial bond between SEBSMA and $nTiO_2$ was excellent because the MA functional groups grafting ethylene butylene of SEBS may react with the -OH group of nanoparticles during melting. The outcomes of DSC of nanocomposites are given in

Table 1. The TPE/5UnTiO_2 nanocomposite with CnTiO_2 has an obvious decrease of crystallization enthalpy (ΔH_C) and melt enthalpy (ΔH_m). This is due to the chemical bonding between TPE and nTiO_2, which inhibits the movement of PBT molecules, thus reducing the crystallization of nanocomposites. Furthermore, the inclusion of TiO_2 nanoparticles in TPE displays a slight effect on the melting temperature (T_m) (Figure 4b). At 5 wt% of TiO_2 nanoparticles, the T_m increases from 208.7 °C of the matrix to 210.1 °C of TPE/5UnTiO_2 nanocomposites. The improvement is about 1.4 °C. The increase in Tm in nanocomposite should be attributed to the chemical bonding between TPE and nTiO_2 in Scheme 1 and the nTiO_2 particle, which introduce an increase in chain length and the molecular weight of TPE. Moreover, the Tm of TPE was improved by the apparent inclusion of CnTiO_2 [Figure 4 (b)]. Take into account the nucleation effect of CnTiO_2 in TPE that the crystallization of TPE in TPE/5CnTiO_2 is mostly measured by CnTiO_2 somewhat by UnTiO_2.

Table 1: Thermal properties of virgin TPE and TPE/nTiO_2 nanocomposites.

Nanocomposites (w/w %)	**T_m (°C)**	**T_c (°C)**	**ΔH_c (J/g)**	**ΔH_m (J/g)**	**T_{onset} (°C) (TGA)**
Virgin TPE	208.7	152.3	30.8	29.6	385.4
TPE/5UnTiO_2	210.1	164.2	28.3	26.7	387.9
TPE/5CnTiO_2	212.3	182.1	27.5	21.8	398.8
TPE/7CnTiO_2	211.8	181.7	26.6	19.3	396.7

The TGA probe provides important evidence in determining the thermal stability of nanocomposites. Thermal stability is a significant property, for which nanocomposite morphology plays an important role [17]. TGA thermograms of virgin TPE and TPE/nTiO_2 nanocomposite are displayed in Figure 5, and the resultant data are recorded in Table 1. It makes sense that all samples demonstrate a one-step decay procedure in the temperature range of 340-460 °C. The weight loss of virgin TPE and its nanocomposite behind 340 °C is less than 0.01% due to outstanding moisture loss in the matrix. In virgin TPE backbone decreases due to the onset decay starting with an acceleration rate from about 340 °C. The onset decay temperature (T_{onset}) of TPE, which gives the thermal stability about 385.4°C. The inclusion of TiO_2 nanoparticles reinforces the thermal stability of TPE, noting that the thermal decay temperature of nanocomposite increases with the concentration of nanoparticles. The most increase in thermal stability for TPE/5CnTiO_2 nanocomposite was 13.4 °C.

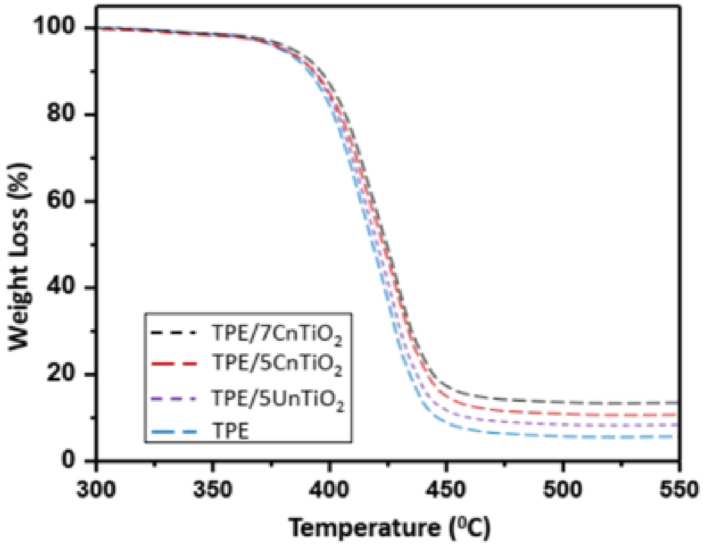

Figure 5: TGA curves of TPE and TPE/nTiO_2 nanocomposites.

Conclusion

The PBT-TEGT block copolymer-based TPE/nTiO$_2$ nanocomposite was manufactured using a melt mixing process tracked by hot press mold. The influences of surface-modified nTiO$_2$ particles on the mechanical, morphological, and thermal features of TPE/nTiO$_2$ nanocomposite were investigated. The inclusion of nTiO$_2$ particles in TPE increased the tensile features of TPE/nTiO$_2$ nanocomposites compared to virgin TPE matrix. Furthermore, the addition of SEBSMA coated-nTiO$_2$ particles to TPE significantly increased the tensile features such as yield strength, tensile strength, and tensile modulus but elongation at break reduced. When the coated-nTiO$_2$ (CnTiO$_2$) was above the 5 wt% rate, the tensile features of the nanocomposites reached their maximum values due to the better interfacial bonding between the TPE and nTiO$_2$ particles available by the MA groups of SEBSMA. SEM tests showed that CnTiO$_2$ was incorporated into TPE, 5CnTiO$_2$ particles were evenly distributed in TPE, and their interface bond with TPE was higher than that of TPE/UnTiO$_2$ in the absence of 5CnTiO$_2$. DSC measurements showed that the inclusion of CnTiO$_2$ resulted in higher crystallization and melting temperatures enriched simultaneously. The crystallization or melting temperature of TPE/5CnTiO$_2$ is much greater than that of TPE/UnTiO$_2$ and that of TPE. The thermal stability of TPE/5CnTiO$_2$ was higher than that of TPE/UnTiO$_2$ because there is a compatibility between TPE and CnTiO$_2$. As a total result of this study, it was sound to confirm that improved morphology, tensile features and, the thermal stability of TPE/nTiO$_2$ or TPE/CnTiO$_2$ were due to the existence of compatibility between TPE and nTiO$_2$ due to a compatibilizer.

Disclosure Statement

The author(s) did not report any potential conflict of interest.

References

1. Gregory GL, Sulley GS, et al. Triblock polyester thermoplastic elastomers with semi-aromatic polymer end blocks by ring-opening copolymerization. Chemical Science. 2020;11:6567-81.
2. Parcheta P, Głowińska E, et al. Effect of bio-based components on the chemical structure, thermal stability and mechanical properties of green thermoplastic polyurethane elastomers. European Polymer Journal. 2020;123:109422.
3. Jiang J, Tang Q, Pan X, Xi Z, Zhao L, Yuan W. Structure and morphology of thermoplastic polyamide elastomer based on long-chain polyamide 1212 and renewable poly (trimethylene glycol). Industrial & Engineering Chemistry Research. 2020;59:17502-12.
4. Zanchin G, Leone G. Polyolefin thermoplastic elastomers from polymerization catalysis: Advantages, pitfalls and future challenges. Progress in Polymer Science. 2021;113:101342.
5. Jiang R, Chen Y, Yao S, Liu T, Xu Z, Park CB, Zhao L. Preparation and characterization of high melt strength thermoplastic polyester elastomer with different topological structure using a two-step functional group reaction. Polymer. 2019;179:121628.
6. Kalfoglou NK. Thermomechanical studies of semicrystalline polyether–ester copolymers. Effect of thermal, mechanical, and solvent treatment. Journal of Applied Polymer Science. 1977;21:543-54.
7. Yao C, Yang G. Crystallization, and morphology of poly (trimethylene terephthalate)/poly (ethylene oxide terephthalate) segmented block copolymers. Polymer. 2010;51:1516-23.
8. Rong MZ, Zhang MQ, Zheng YX, Zeng HM, Friedrich K. Improvement of tensile properties of nano-SiO2/PP composites in relation to percolation mechanism. Polymer. 2001;42:3301-4.
9. 9Džunuzović E, Jeremić K, Nedeljković JM. In situ radical polymerization of methyl methacrylate in a solution of surface modified TiO2 and nanoparticles. European Polymer Journal. 2007;43:3719-26.
10. Kruenate J, Tongpool R, Panyathanmaporn T, Kongrat P. Optical and mechanical properties of polypropylene modified by metal oxides. Surface and Interface Analysis. 2004;36:1044-7.

11. Maiti S, Lopez B. Tensile properties of polypropylene/kaolin composites. Journal of Applied Polymer Science. 1992;44:353-60.
12. Tjong S, Bao S. Fracture toughness of high density polyethylene/SEBS-g-MA/montmorillonite nanocomposites. Composites Science and Technology. 2007;67:314-23.
13. Ishida H, Campbell S, Blackwell J. General approach to nanocomposite preparation. Chemistry of Materials. 2000;12:1260-7.
14. Rahman MT, Hoque MA, Rahman GT, Gafur MA, Khan RA, Hossain MK. Study on the mechanical, electrical and optical properties of metal-oxide nanoparticles dispersed unsaturated polyester resin nanocomposites. Results in Physics. 2019;13:102264.
15. Zaman HU, Hun PD, Khan RA, Yoon KB. Effect of surface-modified nanoparticles on the mechanical properties and crystallization behavior of PP/CaCO3 nanocomposites. Journal of Thermoplastic Composite Materials. 2013;26:1057-70.
16. Ghazy O, Freisinger B, Lieberwith I, Landfester K. Tuning the size and morphology of P3HT/PCBM composite nanoparticles: Towards optimized water-processable organic solar cells. Nanoscale. 2020;12:22798-807.
17. Kilburn D, Dlubek G, Pionteck J, Alam MA. Free volume in poly (n-alkyl methacrylate) s from positron lifetime and PVT experiments and its relation to the structural relaxation. Polymer. 2006;47:7774-85.

- **How to cite this article:** Zaman HU, Khan RA. Mechanical and thermal properties of extruded thermoplastic polyester elastomer/TiO2 nano-composites: effect of surface modification. Advanced Journal of Science and Engineering. 2022;3(2):136-145.
- https://doi.org/10.22034/advjse22032136